Electronic Supplementary Material (ESI) for Journal of Materials Chemistry C.

Electronic Supplementary Information

Crystalline Rubrene by a Novel Process and Realization of a Pyro-phototronic Device with Rubrene based Film

Deepshikha Gogoi[1], Amreen A. Hussain[1,2], Sweety Biswasi[1], Arup R. Pal[1]*

[1] Plasma Nanotech Laboratory, Physical Sciences Division, Institute of Advanced Study in Science and Technology, Paschim Boragaon, Garchuk, Guwahati-781035, India.

[2] Present address: Facilitation Centre for Industrial Plasma Technologies, Institute for Plasma Research, Gandhinagar-382016, Gujarat, India.

[*]Correspondence to: E-mail: arpal@iasst.gov.in (A. R. Pal)

Table S1. Discharge controlling parameters during the deposition of PPA-Amorphous Rubrene (PPA-ARB) and PPA-Crystalline Rubrene (PPA-CRB) samples prepared by using plasma processing method.

Deposition Parameters							
PPA-Amorphous rubrene (ARB)				**PPA- Crystalline rubrene (CRB)**			
p (Torr)	RF Power, P (W)	Negative SB (V)	DT (s)	p (Torr)	RF Power, P (W)	Negative SB (V)	DT (s)
5.0×10^{-2}	10	89	120	5.0×10^{-2}	75	366	40

p = working pressure; P = power; RF = radiofrequency; DT = deposition time; SB = self-bias.

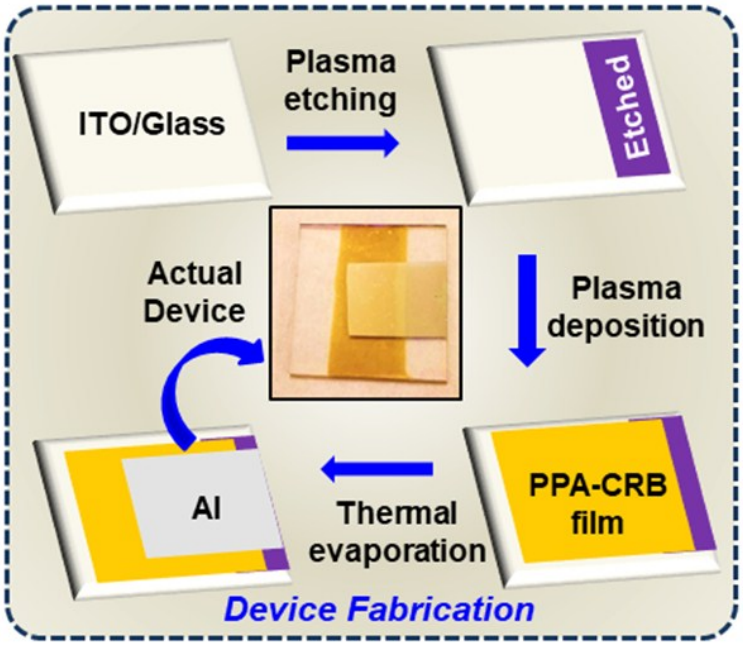

Figure S1. Schematic of the pyro-phototronic device fabrication steps along with an image of the actual device.

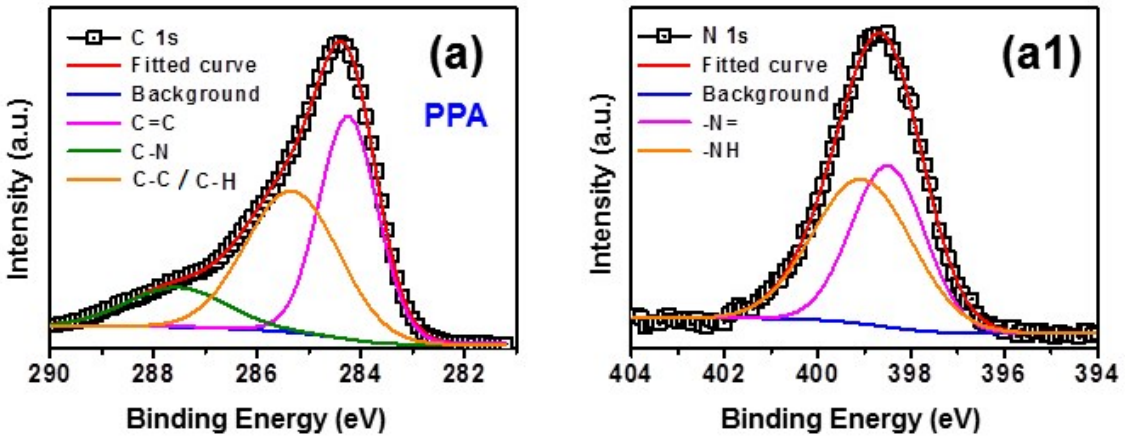

Figure S2. Deconvoluted (a) C1s and (a1) N1s spectra of PPA film.

Table S2. XPS binding energy (BE) positions of PPA, PPA-ARB and PPA-CRB samples with their corresponding BE peak assignments.

Sample	Core Level	Binding Energy (eV)	Assignments[1-3]
PPA	C 1s	284.4 285.2 287.5	C = C C – C / C – H C – N
	N 1s	398.5 399.4	– N = – NH –
PPA-ARB	C 1s	284.5 285.1 285.7	C = C C – C / C – H C = N
	N 1s	398.3 399.4	– N = – NH –
PPA-CRB	C 1s	284.5 285.3	C = C C – C / C – H
	N 1s	398.8 400.1	– N = – NH –

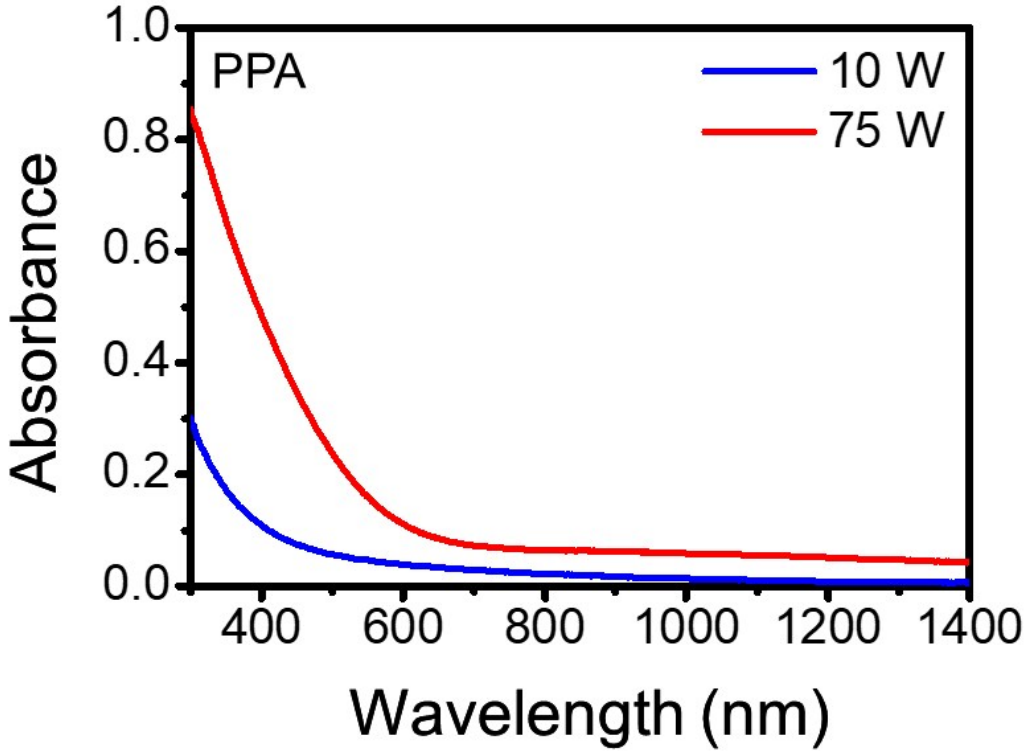

Figure S3. UV-Visible absorbance spectra of PPA at 10 W and 75 W.

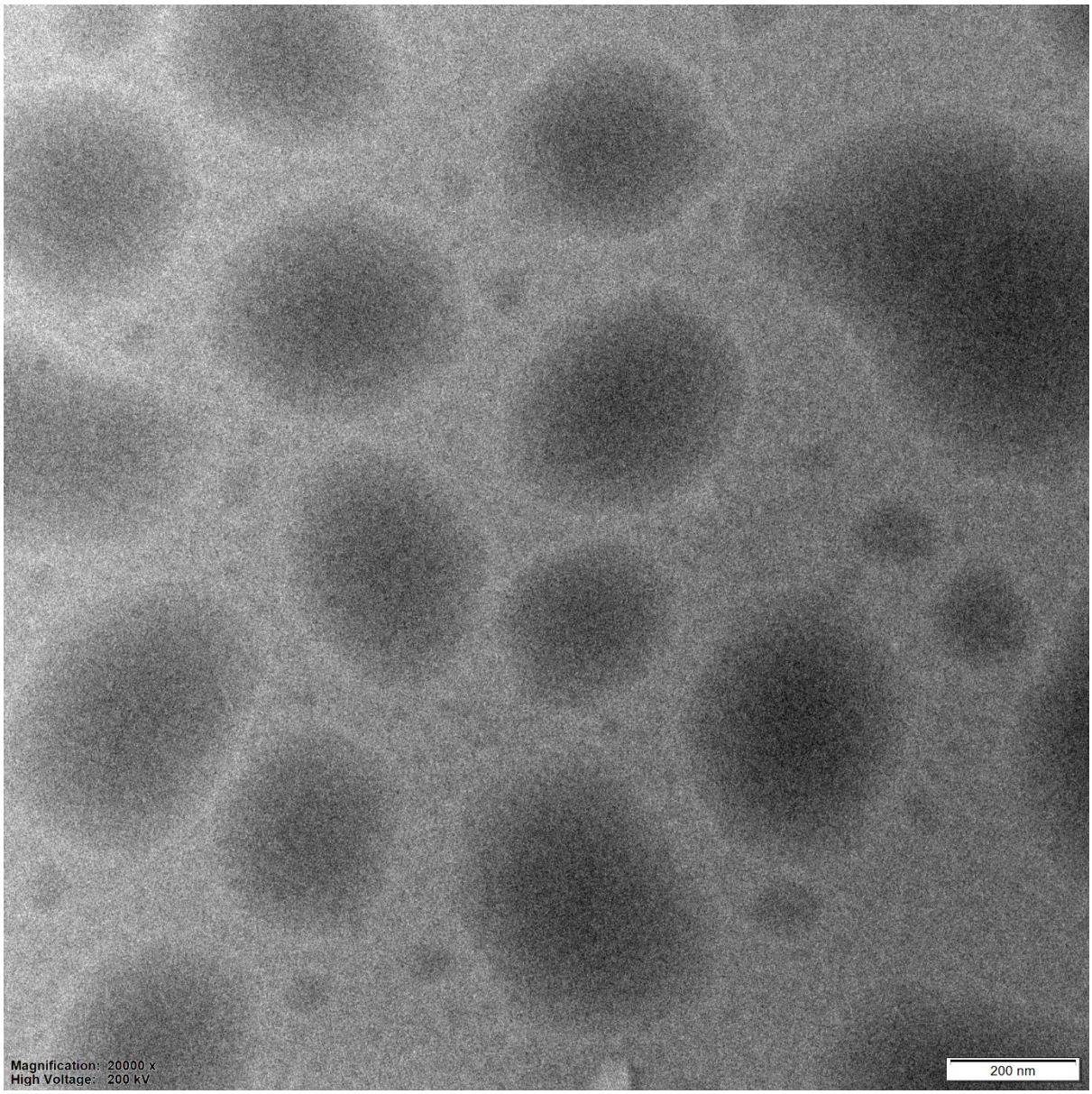

Figure S4. TEM image of the prepared PPA-CRB sample showing deposition of Rubrene crystals, which reveals the deposition of 4×10^8 numbers of crystals per cm^2.

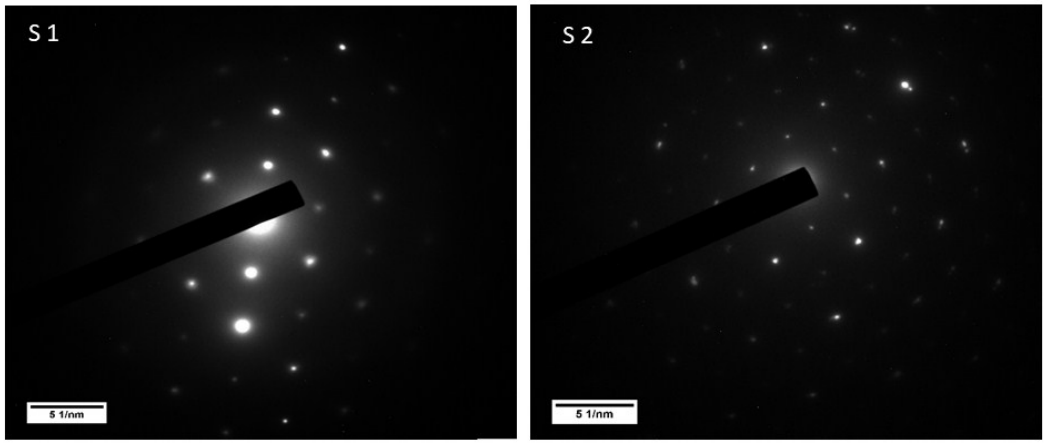

Figure S5. SAED pattern of PPA-CRB showing and confirming the triclinic structure of rubrene crystals in three different directions.

Table S3. Lattice spacing of PPA-CRB samples calculated from SAED pattern and compared to the theoretical triclinic structure of rubrene.
Space Group: Pī

a=0.7326; $\alpha=94.80^0$
b=0.8769; $\beta=106.50^0$
c=1.2298; $\gamma=95.05^0$

Crystal Plane	Lattice spacing (d) nm (Theoritical[2-4])	Lattice spacing (d) nm (Experimental)
022	0.33110	0.33
201	0.31030	0.31
220	0.25750	0.25
222	0.21144	0.21
300	0.23250	0.23

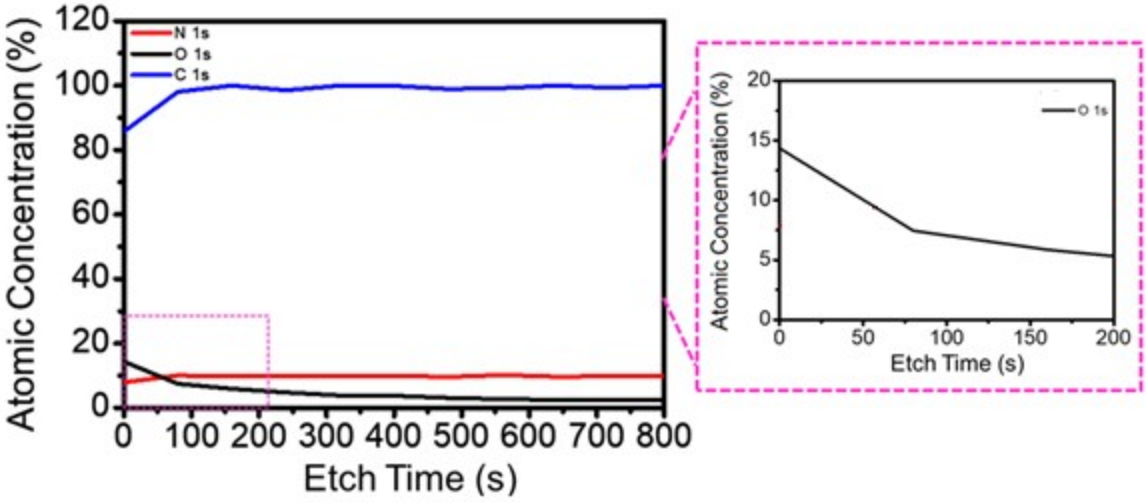

Figure S6. XPS depth profile of PPA-CRB sample etched with an Argon beam energy of 2000 eV. Enlarged data (right panel) shows the presence of significant amount of oxygen at the surface of the film which is responsible for surface polarization.

Table S4. Bias dependence of pyro-phototronic and photovoltaic currents of the PPA-CRB device under the illumination of switching blue light (450 nm) of frequency 0.1 Hz and intensity 1 mW/cm^2.

Applied Bias (Volt)	Pyro-phototronic Current (nA)	Photovoltaic Current (nA)
-1	15	3
-0.5	12	1.7
0	6	0.45
0.5	7.8	0
1	6.4	0.9

References

S1. A. A. Hussain, A. R. Pal, R. Kar, H. Bailung, J. Chutia, D. S. Patil, *Mater. Chem. Phys.* 2014, **148** 540-547.

S2. D. Debarnot, T. Mérian, F. Poncin-Epaillard, *Plasma Chem. Plasma Process.* 2011, **31**, 217-231.

S3. S. Sharma, A. R. Pal, J. Chutia, H. Bailung, N. S. Sarma, N. N. Dass, D. S. Patil, *Appl. Surf. Sci.* 2012, **258**, 2897-7906.

S4. S. Bergantin, M. Moret, *Cryst. Growth Des*. 2012, **12**, 6035-6041.

S5. S. Obata, T. Miura, Y. Shimoi, *Jpn. J. Appl. Phys*. 2014, **53**, 01AD02.

S6. X. Wang, T. Garcia, S. Monaco, B. Schatschneider, N. Marom, *Cryst. Eng. Comm*, 2016, **18**, 7353.